Atmospheric Environment 121 (2015) 86–92

Contents lists available at ScienceDirect

Atmospheric Environment

journal homepage: www.elsevier.com/locate/atmosenv

Sensitivity of global wildfire occurrences to various factors in the context of global change

Yaoxian Huang [a,*], Shiliang Wu [b], Jed O. Kaplan [c]

[a] Department of Geological and Mining Engineering and Sciences, Michigan Technological University, Houghton, MI, USA
[b] Atmospheric Sciences Program, Department of Geological and Mining Engineering and Sciences, Department of Civil and Environmental Engineering, Michigan Technological University, Houghton, MI, USA
[c] Institute of Earth Surface Dynamics, University of Lausanne, Geopolis, Quartier Mouline, 1015 Lausanne, Switzerland

HIGHLIGHTS

- We investigate the potential impacts of global change on wildfire frequencies.
- We account for changing fire meteorology, lightning, population, land use/land cover.
- Fire frequencies are projected to increase by ~27% due to 2000–2050 global change.
- Fire meteorology change is the most important factor, followed by land cover.

ARTICLE INFO

Article history:
Received 5 November 2014
Received in revised form
29 April 2015
Accepted 1 June 2015
Available online 8 June 2015

Keywords:
Wildfire
Land cover/land use
Global change

ABSTRACT

The occurrence of wildfires is very sensitive to fire meteorology, vegetation type and coverage. We investigate the potential impacts of global change (including changes in climate, land use/land cover, and population density) on wildfire frequencies over the period of 2000–2050. We account for the impacts associated with the changes in fire meteorology (such as temperature, precipitation, and relative humidity), vegetation density, as well as lightning and anthropogenic ignitions. Fire frequencies under the 2050 conditions are projected to increase by approximately 27% globally relative to the 2000 levels. Significant increases in fire occurrence are calculated over the Amazon area, Australia and Central Russia, while Southeast Africa shows a large decreasing trend due to significant increases in land use and population. Changes in fire meteorology driven by 2000–2050 climate change are found to increase the global annual total fires by around 19%. Modest increases (~4%) in fire frequency at tropical regions are calculated in response to climate-driven changes in lightning activities, relative to the present-day levels. Changes in land cover by 2050 driven by climate change and increasing CO_2 fertilization are expected to increase the global wildfire occurrences by 15% relative to the 2000 conditions while the 2000–2050 anthropogenic land use changes show little effects on global wildfire frequency. The 2000–2050 changes in global population are projected to reduce the total wildfires by about 7%. In general, changes in future fire meteorology plays the most important role in enhancing the future global wildfires, followed by land cover, lightning activities and land use while changes in population density exhibits the opposite effects during the period of 2000–2050.

1. Introduction

Global wildfire is an important process in the earth system with important implications for climate, atmospheric composition and air quality. The emissions from wildfires contribute significantly to greenhouse gases in the atmosphere (e.g. CO_2 and CH_4), and other trace gases and aerosols, including some air pollutants (e.g. van der Werf et al., 2010; Spracklen et al., 2009). For example, van der Werf et al. (2010) reported that global carbon emissions from wildfires were 1.5–2.8 Pg C yr^{-1} during 1998–2007. As a result, global wildfires can significantly affect the ecosystems, carbon cycle, and climate as well as human health (Bowman et al., 2009; Thelen et al., 2013). On the other hand, the changing climate can significantly affect global wildfire activities by altering fire meteorology (Kloster

* Corresponding author.
E-mail address: yaoxianh@mtu.edu (Y. Huang).

http://dx.doi.org/10.1016/j.atmosenv.2015.06.002
1352-2310/

et al., 2012; Pechony and Shindell, 2010; Marlon et al., 2009).

The occurrence of wildfires is also sensitive to vegetation coverage. Climate change and increasing atmospheric CO_2 fertilization in the coming decades can lead to large perturbations to global vegetation coverage (Wu et al., 2012; Bachelet et al., 2003). For instance, spatial coverage of temperate broadleaf trees in 2100 will increase over 40% (Wu et al., 2012) relative to the year 2000, implying the potential increases in fuel loadings for fire activities in future scenarios. In addition, anthropogenic land use is projected to change significantly on a global scale over the period 2000–2050 (IPCC, 2001). These changes in land use and land cover have important implications for future wildfires by changing the flammability and fuel availability, but these effects have not been well studied in the literature.

Several process-based fire models have been employed to simulate the global fire dynamics (e.g. Krause et al., 2014; Kloster et al., 2012; Li et al., 2012; Pechony and Shindell, 2009, 2010; Arora and Boer, 2005; Thonicke et al., 2001). Thonicke et al. (2001) estimated the fire probability as a function of topsoil moisture and fuel load in the Lund-Potsdam-Jena Dynamic Global Vegetation Model (LPJ DGVM) fire module without explicitly accounting for the ignition sources. Arora and Boer (2005) calculated the probability of fire occurrences in the Canadian Terrestrial Ecosystem Model based on fuel availability, fuel moisture and ignition source. The fire parameterization used in this study follows the scheme developed by Pechony and Shindell (2009) which is a physically based global scale algorithm accounting for the wildfire driving factors from fire meteorology, vegetation density, anthropogenic and natural ignition sources. Pechony and Shindell (2009) have validated this parameterization with satellite observations in terms of both spatial and seasonal variations of wildfire frequencies. Pechony and Shindell (2010) discussed driving factors for global wildfires through changes in climate, land use and population density by the end of the 21st century. This study showed that changes in these factors could lead to increases in future wildfire occurrences by over 25% during 2000–2100 and concluded that future climate may play an even more significant role in shaping global wildfire patterns than anthropogenic-induced ones. Kloster et al. (2012) found that the combined effects from climate, land use and population lead to increases in carbon emissions from global wildfires by up to 62% over the period 1985–2100. Krause et al. (2014) investigated the impacts of future natural ignition source (lightning) changes associated with climate change on global fire occurrence and the resulting burnt area. They found that the global burnt area would increase by 3.3% by the end of the 21st century based on RCP8.5 projection, relative to the present-day conditions. However, none of the previous studies have investigated the impacts on global wildfires from climate-driven changes in land cover.

In this study we investigate the impacts on global wildfires over the period of 2000–2050 from all the major driving factors in the context of global change including (1) changes in lightning activities; (2) changes in fire meteorology including temperature, precipitation and humidity; (3) climate-driven changes in land cover; (4) anthropogenic land use changes; and (5) population density change. We separate these effects through a suite of model sensitivity simulations. A schematic plot regarding the processes and driving factors of the wildfire occurrences is shown in Fig. 1.

2. Method and model description

2.1. Changes in climate, lightning, population density, and land cover/land use

Air surface temperature, precipitation, specific humidity and pressure data were obtained from the GISS GCM 3 at 4° latitude by 5° longitude resolution over the period 2000–2050 (Rind et al., 2007; Wu et al., 2007, 2008a, b; 2012). Relative humidity is calculated offline based on simulated temperature, pressure and specific humidity from GISS GCM 3. Archived meteorology data from GISS GCM 3 was used to drive GEOS-Chem Chemical Transport Model (CTM) (Wu et al., 2007, 2008a, b) to calculate the cloud-to-ground lightning flash rates (natural ignition source) over the 2000–2050 period. Lightning sources are calculated based on computed cloud-top heights (Price and Rind, 1992). For present-day global population density, the Gridded Population of the World Version 3 (GPWv3) was used (CIESIN, 2005), whereas 2050 global population density followed IPCC A1B scenario from Integrated Model to Assess Global Environment (IMAGE) (IMAGE-Team, 2001).

Driven by meteorological fields from the GISS GCM 3, soil data and atmospheric CO_2 concentrations, The LPJ DGVM (Sitch et al., 2003) was used to simulate the 2000–2050 changes in land cover associated with climate change and increasing atmospheric CO_2 fertilization (Wu et al., 2012). The LPJ explicitly simulates fractional density of nine plant function types in every grid cell to examine the land cover changes.

Changes in anthropogenic land use over the period 2000–2050 were from the IMAGE model following the IPCC A1B scenario (IMAGE-Team, 2001; IPCC, 2001; MNP, 2006). More details on the simulation of 2000–2050 land use/land cover change can be found in Wu et al. (2012). We used normalized LAI (by its maxima) as vegetation density for input to our global fire model. To estimate the uncertainty in projected future wildfire frequencies associated with the factor of population density, we also carry out simulations following the IPCC A2 and B1 scenarios for global population densities by 2050s.

To our knowledge, this is the first study on the impacts of global change on wildfires by accounting for all the major factors including the changes in fire meteorology, lightning ignition, population density, as well as land use and land cover. The integrated modeling system used in this study allows us to intercompare the relative importance of various factors as well as their spatiotemporal patterns in the context of global change.

2.2. Fire parameterization

Following Pechony and Shindell (2009), global fire count in each grid box per time step is calculated as

$$N_{fire}(t)_{i,j} = F(t)_{i,j} \times \left(I_N(t)_{i,j} + I_A(t)_{i,j}\right) \times (f_{NS})_{i,j} \quad (1)$$

where N_{fire} is fire count in a time step (t) at a specified longitude (i) and latitude (j) grid box in units of counts per km^2 per month (assuming time step is a month); F is flammability; I_N and I_A are natural ignition source from lightning and anthropogenic ignition source respectively with units of sources per km^2 per month; the fraction of non-suppressed fires (with values ranging between 0 and 1), f_{NS}, is used to account for anthropogenic fire suppression.

Flammability is calculated as

$$F(t)_{i,j} = 10^{Z(T(t)_{i,j})} \times \left(1 - \frac{RH(t)_{i,j}}{100}\right) \times VD(t)_{i,j} \times EXP\left(-c_R R(t)_{i,j}\right) \quad (2)$$

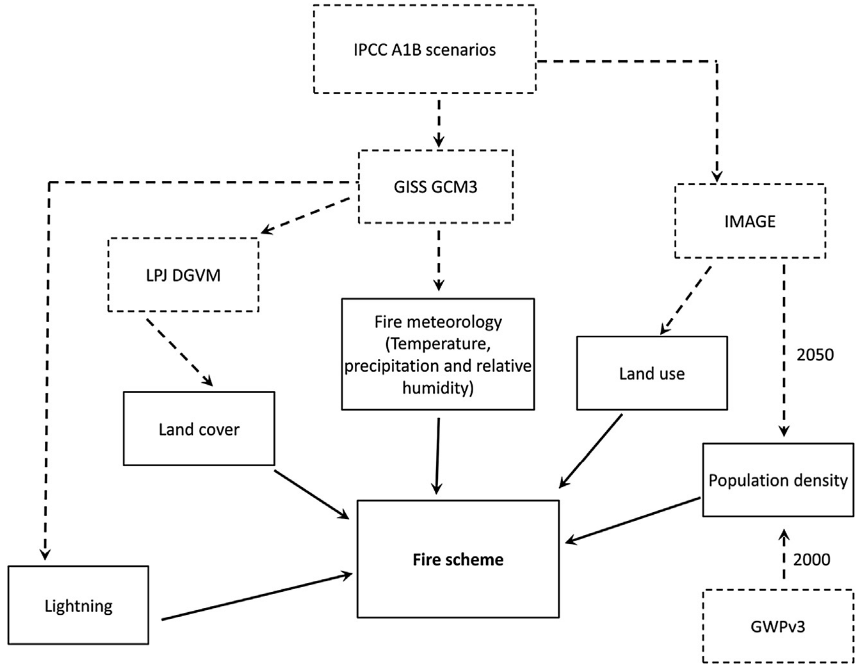

Fig. 1. Schematic plot of the projected 2000–2050 changes in major driving factors (shown in boxes with solid lines) that are used to calculate the wildfire occurrences. Processes on how to calculate changes in these factors are shown in dashed boxes with dashed arrows.

$$Z(T(t))_{i,j} = a\left(\frac{T_s}{T(t)_{i,j}} - 1\right) + b \times \log\left(\frac{T_s}{T(t)_{i,j}}\right) + c \times \left(10^{d\times\left(1-\frac{T_s}{T(t)_{i,j}}\right)} - 1\right) + f\left(10^{h\times\left(\frac{T_s}{T(t)_{i,j}}-1\right)} - 1\right) \tag{3}$$

where RH and T are surface air relative humidity (in %) and temperature (in K) respectively; VD is vegetation density coefficient; R is surface mean precipitation (mm/day) and $c_R = 2$ (day/mm); $Z(T(t))_{i,j}$ is expressed in Eq. (3), which is used to calculate vapor pressure deficit (Goff and Gratch, 1946) together with relative humidity; The constants in Eq. (3) are: a = −7.90298; water boiling temperature T_s=373.16(°K); b = 5.02808; c = -1.3816×10^{-7}; d = 11.344; f = 8.1328×10^{-3}; h = −3.49149.

Anthropogenic ignition source and fraction of non-suppressed fires are both calculated as a function of population density, which are shown as

$$I_A = k(PD) \times PD \times \delta \tag{4}$$

$$f_{NS} = c_1 + c_2 \times EXP(-\omega \times PD) \tag{5}$$

where PD is the population density (persons per km^2); the term $k(PD) = 6.8PD^{-0.6}$ is used to represent the variable ignition potentials in a region with different population densities; δ (= 0.03) is the number of potential ignition sources per person per month per km^2; Constant values in Eq. (5) are: $c_1 = 0.05$, $c_2 = 0.9$, $\omega = 0.05$.

We run the model from 1998 to 2002 for present-day conditions at the resolution of 4° × 5° (latitude x longitude) at a temporal resolution of one month. For future scenario, we run the model from 2048 to 2052. To separate the effect on future fire occurrence associated with various factors, we performed a suite of model experiments by perturbing only one single factor at a time while keeping other variables under present-day conditions. For instance, in order to investigate the fire performance in response to future changes in lightning only, we conducted sensitivity test by only changing lightning source to future scenario while keeping other parameters as present-day values.

3. Results and discussions

For the present-day conditions, our model results successfully reproduce the spatial variability of wildfires, with highest fire frequencies in Africa and South America, which are generally consistent with MODIS observations and Pechony and Shindell (2009). In order to validate our model performance, we used MODIS/Terra monthly Active Fire Product V004 (MOD14CM1) at resolution of 1° × 1° (Leptoukh et al., 2007) to compare with our present-day model output. To better compare the modeled fire counts with MODIS products, we use normalized fire counts for model results and MODIS data. The normalized fire count is the ratio of the annual fire count at a given location to the global maximum annual fire count. Fig. 2 shows the scatter plots between normalized model (1998–2002) and MODIS (2001–2005) fire frequencies spanning from the global scale to regions including South America, Africa and Australia. Due to the lack of data from MODIS during 1998–2000, 2001–2005 annual average fire frequencies from MODIS are used instead to compare with our model results. The global correlation coefficient between model and MODIS is r = 0.53. For South America, Africa and Australia, the correlation coefficients are 0.73, 0.66 and 0.60 respectively, which are comparable to Pechony and Shindell (2009), with r = 0.77. Lower r value in our result is partly caused by coarser model resolutions and different meteorological datasets used. Some systematic high bias is observed with the model results, in particular over South America. This may partly reflects the likely low bias of the MODIS products. As discussed by Wiedinmyer et al. (2011), the MODIS instrument on board the Terra polar orbiting satellites operates in a low earth orbit and has a twice-a-day sampling frequency. Therefore the operational swath

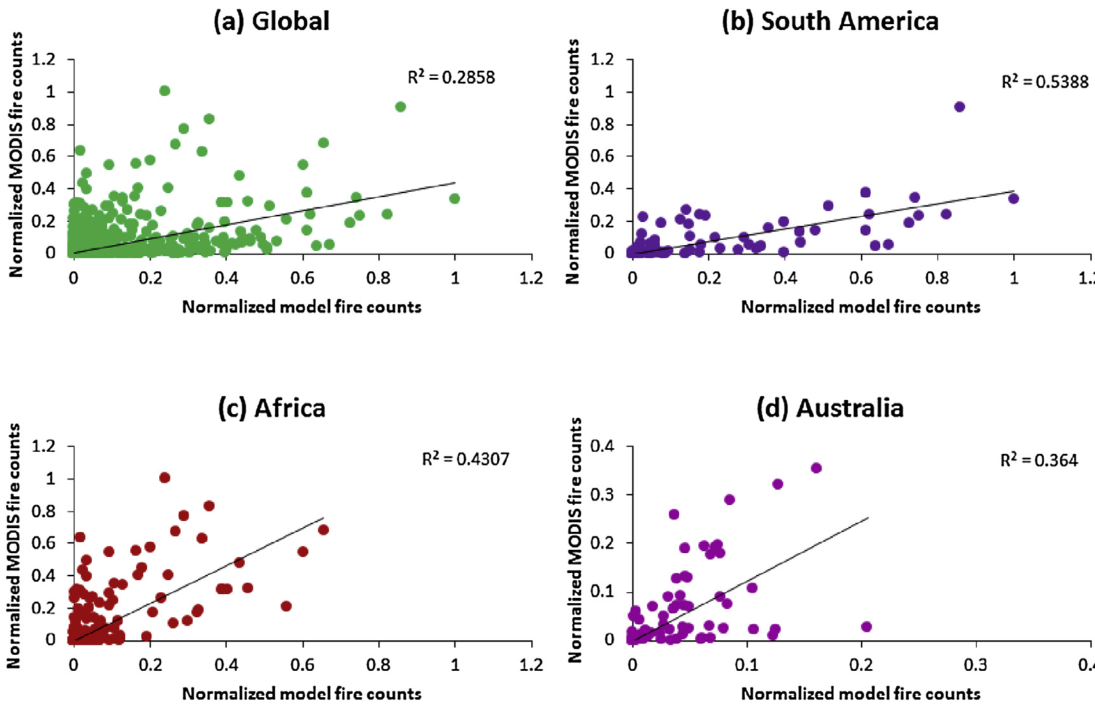

Fig. 2. Scatter plots of annual mean model (1998–2002) and MODIS fire frequencies (2001–2005) in collocated (a) global (b) South America (c) Africa (d) Australia grid boxes. Solid line shows least square linear fit, with correlation coefficients (R^2) shown for each panel.

path does not cover the entire globe daily at lower latitudes (latitudes between 30°N and 30°S) and fires can be missed. In addition, the coarse model resolution could also contribute to the model bias. Due to the relatively coarse resolution, our model is not able to resolve the fire occurrences at local scale.

Fig. 3 shows the projected changes of fire frequencies in response to 2000–2050 changes in various factors including lightning, climate, land cover, land use, and population as well as all combined effects. The changes in lightning activities lead to an increase in global fire frequency by ~4%, with significant increases over tropical and some northern mid-high latitude regions (Fig. 3a). This is consistent with the study by Krause et al. (2014), which showed that global burnt area driven by changes in lightning will increase by up to ~3.3% by the end of the 21st century following the RCP8.5 scenario. Largest increases are found over the Amazon regions.

The perturbations to fire frequencies from changes in lightning activities over the 2000–2050 period show significant seasonal variations (Fig. 4a). For the Northern Hemisphere, the impacts from lightning changes peak in June-August when the total fire frequencies increase by ~3.6%. During summertime, the increases in lightning ignition sources at mid-high latitudes play an important role in strengthening the boreal wildfire activities (e.g. Russian regions). For the Southern Hemisphere, the largest impacts are calculated for September–November with the total fire frequencies increase by ~11.5%. Fire regimes over continents in the Southern Hemisphere increase the largest in this season.

Driven by 2000–2050 changes in fire meteorology (T, P and RH), global fire frequency increases by approximately 19%, compared to the present-day level (Fig. 3b). This is consistent with previous studies which showed that changes in climate could lead to significant increases in wildfires, and hence fire emissions in future climate scenarios (Kloster et al., 2012; Pechony and Shindell, 2010). For instance, Kloster et al. (2012) calculated that, driven by climate change following IPCC A1B scenario, fire emissions would increase by up to 22% by the end of the 21st century relative to the preindustrial era. As discussed in Wu et al. (2008b), the global annual mean surface temperature is projected to increase by ~ 1.8 K driven by 2000–2050 climate change following the IPCC A1B scenario. The flammability as calculated by Eq. (2) is very sensitive to temperature perturbation. Generally, higher temperature leads to higher flammability due to increases in vapor pressure deficit, thus enhancing the fire occurrences.

Future changes in precipitation play a key role in affecting the future trend in fire frequencies. Significant increases of precipitation are projected over the tropical regions and high latitudes of Northern Hemisphere while large decreases are found over the Western United States, Eastern Australia, Northern and Southern Africa. As a result, significant increases of fire frequencies are simulated over South America, most regions of Africa and Eastern Australia, whereas Western Russia, Central Africa and west of South America show decreasing trends (Fig. 3b).

Fig. 4b shows the projected changes in fires in response to fire meteorology changes for various seasons. For the Northern Hemisphere, wintertime fire frequencies increase by approximately 36.7% compared to present, mainly in tropical Africa. Fire frequencies in boreal spring, summer and fall increase by 23.5%, 12% and 9.9% respectively, compared to the 2000 seasons. For the Southern Hemisphere, we find that largest increases in fire frequencies are calculated in the austral summer (December-February), with fire increases about 39.7%, relative to present. Relative to the 2000 seasons, fire frequencies in spring, fall and winter increase by 19%, 18.3% and 17.4% respectively. Some regions even show contrasting trends for different seasons. For example, compared to present, fire frequencies in the southern part of South America show a reduction in austral autumn but increases in austral winter and spring.

Fig. 3c represents changes in global fire occurrence due to land cover (vegetation) changes, with global fire frequencies increases by ~ 15% between the present-day and future conditions, which is comparable to the impacts from fire meteorology factor. Significant

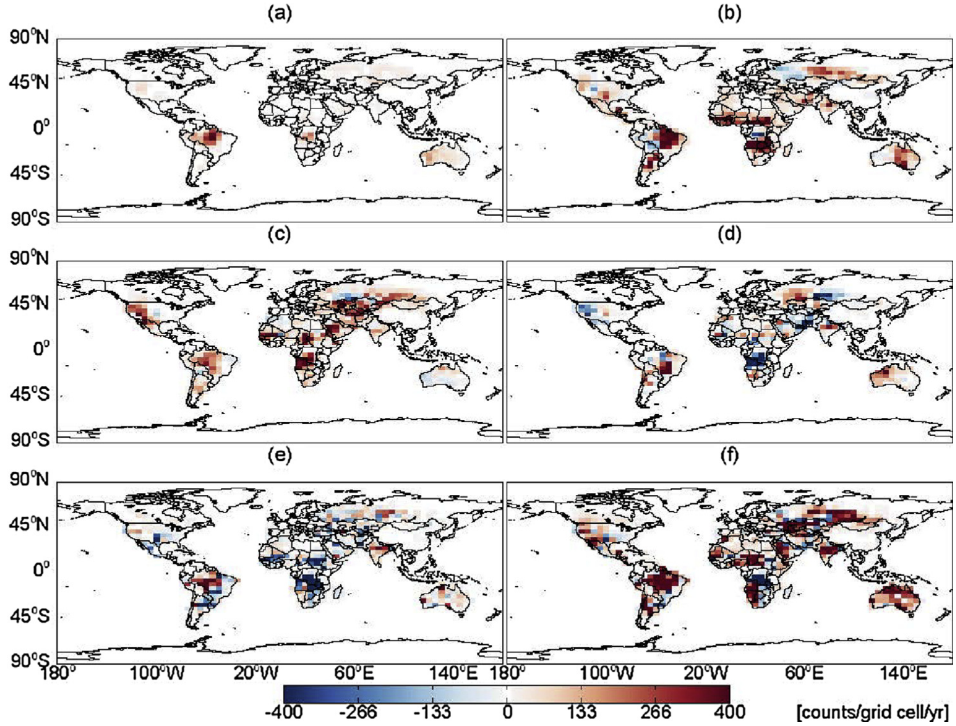

Fig. 3. Projected annual mean 2000–2050 changes in fire frequencies in response to 2050 (a) lightning (b) climate (c) land cover (d) land use (e) population density (f) all combined factors from a-e.

increases are found over Africa, Western United States and Northern Mexico. General increases in LAI are calculated by the LPJ model except for the subtropics, which leads to increases in global fire frequencies. Additionally, global warming and poleward expansions of forests result in increases in LAI over high latitudes (Tai et al., 2013; Wu et al., 2012). As a consequence, wildfire frequency and burned area may extend poleward during summertime (e.g. boreal wildfires), with significant implications for Arctic air

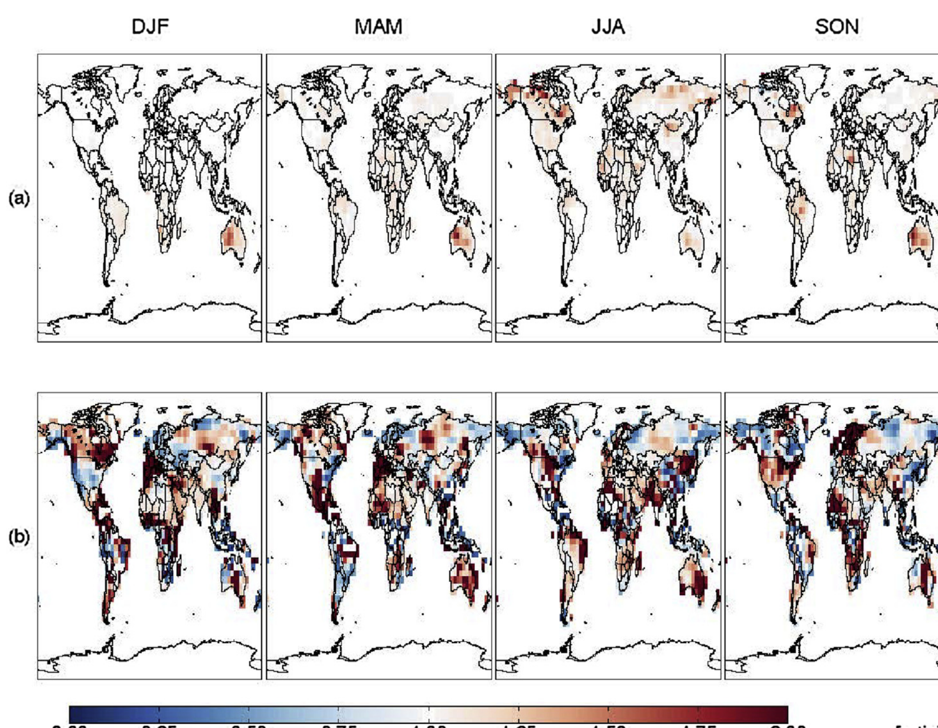

Fig. 4. Ratio plot for projected seasonal fire frequencies changes between the 2000 and 2050 scenarios in response to changes in 2050 (a) lightning (b) climate in DJF (first column), MAM (second column), JJA (third column) and SON (last column) respectively. Ratio is represented as future fire frequencies over present-day level.

pollution in the future. By contrast, fires in West Russia show a decreasing trend, which is caused by the reduction coverage of boreal summergreen and/or needleleaved evergreen tree (Wu et al., 2012), thus lowering the fire frequency in this region.

Changes in global fire occurrence due to future changes in land use are shown in Fig. 3d. Anthropogenic land use is projected to increase in area over Central Africa, Central Russia, the Middle East and Western United States but decrease in other regions such as South America, West Australia and West Russia (IPCC, 2001; MNP, 2006). The 2000–2050 changes in land use are expected to have negligible effects on the global total fire occurrences. However, some significant regional effects are simulated. For instance, strong increases in fire frequency are found over Western Russia, South America and West Australia whereas large decreases in fire frequency occur in the Western United States, Central Africa, West Asia and Central Russia.

Fig. 3e shows the perturbations to fire frequencies resulting from future anthropogenic ignition and suppression changes associated with the expected population changes following the IPCC A1B scenario. The global total fire frequencies are calculated to decrease by ~7% in 2050s. This is consistent with the study by Kloster et al. (2012) who reported that global fire carbon emissions decreased by ~ 6% in response to global population density changes. The largest reductions in fire frequency are found over Africa, reflecting the significant increases in population density there and therefore enhanced fire suppression in these regions in the future. On the other hand, wildfires are projected to increase in frequency over the Amazon and in Australia, driven by the increases in human-induced ignition sources associated with slight increases in population density. These regions have relatively low population density and the unsuppressed ignition sources (the product of $I_A f_{NS}$ as calculated in Eq. (1)) would increase with the population density (PD). This is in contrast to the case of Africa discussed above where the population density is high and the number of unsuppressed ignition sources would decrease with population density. Our sensitivity model simulations also show that if the global population densities follow the IPCC A2 or B1 scenarios instead, the global fire frequencies would reduce by 6% and 10% respectively, compared with the present-day levels.

Taking into account all the factors in the context of global change (changes in lightning, fire meteorology, land cover, land use and population) following IPCC A1B scenarios, we find that the global fire frequencies in 2050s would increase by approximately 27% compared to the first decade of the 21st century (Fig. 3f). Future changes in lightning activity, fire meteorology and land cover all contribute to the increasing fire occurrences while changes in population and land use lead to reductions of fires. Significant fire increases are simulated over regions including the Western United States, South America, Northern Africa, Central Russia and Australia, while decreases are calculated over regions such as Southeast Africa, mainly due to increases in land use and population growth. On the global scale, changes in fire meteorology and land cover appear to be the most important factors affecting the future evolution of wildfire frequency.

There are significant uncertainties with the projected wildfire activities in the future but it's very difficult to quantify the uncertainty associated with each factor (such as the simulated meteorology, vegetation and population density). For example, the future population density varies significantly among various IPCC scenarios (such as A2, A1B and B1). The A2 scenario has the highest predicted global population density in 2050s, which could lead to a 10% decrease in the future global fire frequency due to anthropogenic suppression effect, while the A1B and B1 scenarios are calculated to decrease the global fire frequency by 7% and 6% respectively by 2050s.

4. Conclusions

We investigate the impacts on future global wildfire occurrences associated with major driving factors in the context of global change including fire meteorology, vegetation density, as well as lightning and anthropogenic ignitions. Compared to the 2000 conditions, the global fire frequencies in 2050s are simulated to increase by about 27% when changes in all driving factors are considered. Climate-driven changes in lightning activities and fire meteorology (including temperature, precipitation and humidity) over the period 2000–2050 increase the global fire occurrences by approximately 4% and 19% respectively. The 2000–2050 changes in global population are expected to reduce the global total wildfire occurrences by around 7%. Driven by climate change and increasing CO_2 fertilization, changes in land cover by 2050 are calculated to increase global wildfires by about 15% compared to the 2000 levels. In contrast, we find that the 2000–2050 changes in land use result in little effects on global total wildfire occurrences but large perturbations for some regions. Significant increases in fire occurrence are simulated over the Amazon area, Australia and Central Russia primarily driven by changes in lightning activities, fire meteorology and land cover while a large decreasing trend is projected over the Southeast Africa due to changes in land use and population.

Acknowledgement

We thank Dr. Olga Pechony for very helpful discussions and providing us the 2050s population dataset from IMAGE. This publication was made possible by a U.S. EPA grant (grant 83518901). Its contents are solely the responsibility of the grantee and do not necessarily represent the official views of the U.S. EPA. Further, U.S. EPA does not endorse the purchase of any commercial products or services mentioned in the publication. S. Wu acknowledges support from the National Science Foundation (grant #1313755). Superior, a high performance computing cluster at Michigan Technological University, was used in obtaining results presented in this publication.

References

Arora, V.K., Boer, G.J., 2005. Fire as an interactive component of dynamic vegetation models. J. Geophys. Res. 110, G02008. http://dx.doi.org/10.1029/2005JG000042.

Bachelet, D., Neilson, R.P., Hickler, T., Drapek, R.J., Lenihan, J.M., Sykes, M.T., Smith, B., Sitch, S., Thonicke, K., 2003. Simulating past and future dynamics of natural ecosystems in the United States. Global Biogeochem. Cycles 17, 1045. http://dx.doi.org/10.1029/2001GB001508.

Bowman, D.M.J.S., Balch, J.K., Artaxo, P., Bond, W.J., Carlson, J.M., Cochrane, M.A., D'Antonio, C.M., DeFries, R.S., Doyle, J.C., Harrison, S.P., Johnston, F.H., Keeley, J.E., Krawchuk, M.A., Kull, C.A., Marston, J.B., Moritz, M.A., Prentice, I.C., Roos, C.I., Scott, A.C., Swetnam, T.W., van der Werf, G.R., Pyne, S.J., 2009. Fire in the earth system. Science 324, 481–484. http://dx.doi.org/10.1126/science.1163886.

Center for International Earth Science Information Network (CIESIN), 2005. Gridded Population of the World Version 3 (GPWv3): Population Density Grids, Palisades, NY, Socioecon. Data and Appl. Cent. (SEDAC), Columbia Univ., New York (Available at: http://sedac.ciesin.columbia.edu/gpw.

IMAGE-Team, 2001. The IMAGE 2.2 implementation of the SRES scenarios: a comprehensive analysis of emissions. In: Climate Change and Impacts in the 21st Century, RIVM CD-rom Publication 481508018. Natl. Inst. for Public Health & the Environment, Bilthoven.

IPCC: Climate Change, 2001. In: Houghton, J.T., Ding, Y., Griggs, D.J., Noguer, M., van der, P.J.L., Dai, X., Maskell, K., Johnson, C.A. (Eds.), The Scientific Basis, Contribution of Working Group I to the Third Assessment Report of the Intergovernmental Panel on Climate Change. Cambridge University Press, Cambridge, United Kingdom and New York, NY, USA, p. 881.

Kloster, S., Mahowald, N.M., Randerson, J.T., Lawrence, P.J., 2012. The impacts of climate, land use and demography on fires during the 21st century simulated by CLM-CN. Biogeosciences 9, 509–525. http://dx.doi.org/10.5194/bg-9-509-2012.

Krause, A., Kloster, S., Wilkenskjeld, S., Paeth, H., 2014. The sensitivity of global wildfires to simulated past, present, and future lightning frequency. J. Geophys. Res. Biogeosci. 119 http://dx.doi.org/10.1002/2013JG002502.

Leptoukh, G., Csiszar, I., Romanov, P., Shen, S., Loboda, T., Gerasimov, I., 2007. NASA

NEESPI data and services center for satellite remote sensing information. Environ. Res. Lett. 2, 045009–045015. http://dx.doi.org/10.1088/1748-9326/2/4/045009.
Li, F., Zeng, X.D., Levis, S., 2012. A process-based fire parameterization of intermediate complexity in a dynamic global vegetation model. Biogeosciences 9, 2761–2780. http://dx.doi.org/10.5194/bg-9-2761-2012.
Marlon, J.R., Bartlein, P.J., Walsh, M.K., Harrison, S.P., Brown, K.J., Edwards, M.E., Higuera, P.E., Power, M.J., Anderson, R.S., Briles, C., Brunelle, A., Carcaillet, C., Daniels, M., Hu, F.S., Lavoie, M., Long, C., Minckley, T., Richard, P.J.H., Scott, A.C., Shafer, D.S., Tinner, W., Umbanhowar, C.E., Whitlock, C., 2009. Wildfire responses to abrupt climate change in North America. Proc. Natl. Acad. Sci. U. S. A. 106, 2519–2524. http://dx.doi.org/10.1073/pnas.0808212106.
MNP, 2006. In: Bouwman, A.F., Kram, T., Klein Goldewijk, K. (Eds.), Integrated Modeling of Global Environmental Change, an Overview of IMAGE 2.4. Netherlands Environmental Assessment Agency (MNP), Bilthoven, The Netherlands.
Pechony, O., Shindell, D.T., 2009. Fire parameterization on a global scale. J. Geophys. Res. Atmos. 114, D16115. http://dx.doi.org/10.1029/2009JD011927.
Pechony, O., Shindell, D.T., 2010. Driving forces of global wildfires over the past millennium and the forthcoming century. Proc. Natl. Acad. Sci. U. S. A. 107, 19167–19170. http://dx.doi.org/10.1073/pnas.1003669107.
Price, C., Rind, D., 1992. A simple lightning parameterization for calculating global lightning distributions. J. Geophys. Res. 97, 9919–9933. http://dx.doi.org/10.1029/92JD00719.
Rind, D., Lerner, J., Jonas, J., McLinden, C., 2007. Effects of resolution and model physics on tracer transports in the NASA Goddard Institute for Space Studies general circulation models. J. Geophys. Res. Atmos. 112, D09315. http://dx.doi.org/10.1029/2006JD007476.
Sitch, S., Smith, B., Prentice, I.C., Arneth, A., Bondeau, A., Cramer, W., Kaplan, J.O., Levis, S., Lucht, W., Sykes, M.T., Thonicke, K., Venevsky, S., 2003. Evaluation of ecosystem dynamics, plant geography and terrestrial carbon cycling in the LPJ dynamic global vegetation model. Global Change Biol. 9, 161–185.
Spracklen, D.V., Mickley, L.J., Logan, J.A., Hudman, R.C., Yevich, R., Flannigan, M.D., Westerling, A.L., 2009. Impacts of climate change from 2000 to 2050 on wildfire activity and carbonaceous aerosol concentrations in the western United States. J. Geophys. Res. 114, D20301. http://dx.doi.org/10.1029/2008JD010966.
Tai, A.P.K., Mickley, L.J., Heald, C.L., Wu, S., 2013. Effect of CO_2 inhibition on biogenic isoprene emission: implications for air quality under 2000 to 2050 changes in climate, vegetation, and land use. Geophys. Res. Lett. 40, 3479–3483. http://dx.doi.org/10.1002/grl.50650.
Thelen, B., French, N.H.F., Koziol, B.W., Billmire, M., Owen, R.C., Johnson, J., Ginsberg, M., Loboda, T., Wu, S., 2013. Modeling acute respiratory illness during the 2007 San Diego wildland fires using a coupled emissions-transport system and generalized additive modeling. Environ. Health 12, 94. http://dx.doi.org/10.1186/1476-069X-12-94.
Thonicke, K., Venevsky, S., Sitch, S., Cramer, W., 2001. Global Ecol. Biogeogr. 10, 661–667.
van der Werf, G.R., Randerson, J.T., Giglio, L., Collatz, G.J., Mu, M., Kasibhatla, P.S., Morton, D.C., DeFries, R.S., Jin, Y., van Leeuwen, T.T., 2010. Global fire emissions and the contribution of deforestation, savanna, forest, agricultural, and peat fires (1997-2009). Atmos. Chem. Phys. 10, 11707–11735. http://dx.doi.org/10.5194/acp-10-11707-2010.
Wiedinmyer, C., Akagi, S.K., Yokelson, R.J., Emmons, L.K., Al-Saadi, J.A., Orlando, J.J., Soja, A.J., 2011. The Fire INventory from NCAR (FINN): a high resolution global model to estimate the emissions from open burning. Geosci. Model Dev. 4 (3), 625–641. http://dx.doi.org/10.5194/gmd-4-625-2011.
Wu, S., Mickley, L.J., Jacob, D.J., Rind, D., Streets, D.G., 2008a. Effects of 2000-2050 changes in climate and emissions on global tropospheric ozone and the policy-relevant background surface ozone in the United States. J. Geophys. Res. Atmos. 113, D18312. http://dx.doi.org/10.1029/2007JD009639.
Wu, S., Mickley, L.J., Kaplan, J.O., Jacob, D.J., 2012. Impacts of changes in land use and land cover on atmospheric chemistry and air quality over the 21st century. Atmos. Chem. Phys. 12, 1597–1609. http://dx.doi.org/10.5194/acp-12-1597-2012.
Wu, S., Mickley, L.J., Leibensperger, E.M., Jacob, D.J., Rind, D., Streets, D.G., 2008b. Effects of 2000-2050 global change on ozone air quality in the United States. J. Geophys. Res. Atmos. 113, D06302. http://dx.doi.org/10.1029/2007JD008917.
Wu, S., Mickley, L.J., Jacob, D.J., Logan, J.A., Yantosca, R.M., Rind, D., 2007. Why are there large differences between models in global budgets of tropospheric ozone? J. Geophys. Res. Atmos. 112, D05302. http://dx.doi.org/10.1029/2006JD007801.